Brazing developments of SiC-based E-ATF fuel rods for LWR

Valérie Chaumat, Christophe Lorrette, Thorsten Marlaud

BRAZING DEVELOPMENTS OF SIC-BASED E-ATF FUEL RODS FOR LWR

V. CHAUMAT
Univ. Grenoble Alpes, CEA, Liten, DTCH,
38000 Grenoble, France

C. LORRETTE
Université Paris-Saclay, CEA, Service de Recherches en Matériaux et procédés Avancés,
91191, Gif-sur Yvette, France

T. MARLAUD
Framatome, Fuel Design, 2 Rue Professeur Jean Bernard,
69007 Lyon, France

ABSTRACT

This paper presents recent achievements in joining methods developed for the closure of tubular CVI-SiC_f/SiC composites considered as cladding solution for Light Water Reactor (LWR) fuel rods. This study was conducted as part of a collaboration between Framatome and CEA (Commissariat à l'Energie Atomique et aux Energies Alternatives). Based on CEA non-reactive BraSiC® process, various brazing systems were investigated. X-ray tomography of the BraSiC® joints showed satisfactory filling by the braze. Mechanical "push out" tests and destructive characterizations (cross sections for optical and SEM observations) were conducted before and after hydrothermal corrosion testing in an autoclave at 360°C and 187 bars in LWR water conditions. The results depend on the composition of the BraSiC® brazes and demonstrate the relevance of BraSiC® process for SiC-based E-ATF fuel rods for LWR.

1. Introduction

Following the Fukushima event, the global nuclear industry accelerated research into Enhanced-Accident Tolerant Fuel (E-ATF). As part of its PROtect[1]-SiC program, Framatome is cooperating with CEA to develop SiC_f/SiC fuel rods, as a long-term solution, aimed to offer drastic improvements during beyond design basis accidents in GEN III/III+ LWRs. SiC_f/SiC composites offers outstanding dimensional stability and mechanical integrity when reaching accidental temperatures while exhibiting low interaction with steam.

Several critical technical challenges need to be overcome to consider CVI-manufactured SiC_f/SiC composite as cladding solution for LWRs (e.g., hydrothermal corrosion, fission product hermeticity and joining method). To address these challenges, CEA and Framatome are collaborating on an innovative design [1], consisting of an Environment Barrier Coating (EBC) on the outer surface to prevent Si recession, a SiC_f/SiC composites structural layer and a thin metallic liner inside the composite structure to ensure hermiticity [2], [3]. This multilayer design is mature enough for irradiation programs (like ongoing MITR and ATR irradiation program) and efforts are continuing to increase the maturity of the full size fuel rod design.

[1] PROtect is a trademark or registered trademark of Framatome or its affiliates, in the USA or other countries

In the present work, brazing is investigated as a joining method to close tubular CVI-SiC_f/SiC composites. Based on CEA's non-reactive BraSiC® process [4], [5], [6], various brazing systems were considered as joining material in a representative geometry. This method uses silicon and/or silicide-based alloys (BraSiC® alloys) that do not react with the SiC (absence of reactions products at the interface braze / SiC until the atomic scale has been demonstrated in [7]). This compatibility is a real advantage over other refractory brazing alloys that react strongly with SiC and form brittle compounds that lead to weak interfaces and joints [8], [9]. Therefore, the SiC / BraSiC® / SiC joints are robust and some BraSiC® alloys have already been qualified for space applications [10]. They have also been specified for fuel cladding assemblies in GFRs (Gas-cooled Fast Reactors) [11].
While the hydrothermal corrosion of SiC_f/SiC composites in LWR conditions has been the subject of several studies, the corrosion performance of brazed joints needs further investigation. Consequently, BraSiC® alloy brazed joints and SiC_f/SiC samples coated with BraSiC® alloys have been exposed to LWR conditions, with the objective of understanding their corrosion behaviour and mechanical properties after exposure. At a first step, the study focus on the reference BraSiC® braze Si-Zr alloy already specified for GFR but not LWR (referenced alloy #1 in this work) through mechanical tests before and after exposure in autoclave of as-brazed tube/cap joints, and autoclave of a representative rodlet brazed with alloy #1 and protected by EBC. In a second phase, a corrosion screening tests in autoclave of samples brazed or coated with different BraSiC® alloys had been performed with the objective of identifying novel and robust brazing solutions for use in LWRs.

2. Materials and experimental methods

The CVI-SiC_f/SiC composite was manufactured by CEA. This material consists of SiC fiber reinforcement within a SiC matrix introduced by chemical vapour infiltration (CVI). High-performance third-generation Hi-Nicalon type S (NGS Advanced Fibers Co., LTD Toyama-Shi, Japan) fibers were infiltrated with a thin pyrocarbon (PyC, 30-100 nm) layer followed by SiC matrix. The PyC layer allows the cracks deflection at the fiber/matrix interface and confers the damageable behaviour of the ceramic. After infiltration, the inner and outer surfaces of the tubes were ground as the last step of the manufacturing process. More details are given in reference [12].

Three types of samples were prepared by brazing tubes (representative LWRs fuel cladding dimensions, diameters ext 9.50 – int 8.36 mm) in different configurations:

With reference BraSiC® braze Si-Zr alloy (alloy #1):

- **Configuration A for mechanical tests of the as-brazed tube/cap joints before and after hydrothermal corrosion testing:** Tubes closed with end-caps at one side (Figure 1a) by brazing with alloy #1 (Si-Zr system)**;**
- **Configuration B for hydrothermal corrosion testing of EBC-protected rodlet:** Representative rodlets constituted of tubes brazed with end-caps at both sides (Figure 1b) using alloy #1. A finishing surface treatment was realized after brazing to remove excess brazed material and produce representative and smooth surfaces of cladding tubes. An EBC was applied to the finished surface.

With different BraSiC® braze compositions:

- **Configuration C for corrosion screening tests: Tube samples** with different BraSiC® braze compositions and brazing conditions. Table 1 lists the alloy types and brazing temperatures. Two sub-configurations (depicted Figure 2) were used: CVI-SiC_f/SiC tubes coated by the brazing alloy (Type I), and CVI-SiC_f/SiC inner tubes brazed to an outer sintered SiC tube (thickness of the joint ~ 200 µm, Type II).

Brazing was carried out under vacuum in a furnace at CEA. The brazing temperature for each alloy is given in Table 1. The brazing conditions were optimized for each alloy through wetting experiments that are not detailed here. For temperatures higher than 1500°C, brazing was performed under argon to limit evaporation. All the samples prepared are listed in Table 2.

Table 1: Braze references and brazing temperatures.

Systems	**Si-Zr**		**Si-Cr**		**Si-Ti**	**Si-Y**
Alloy references	#1	#2	#3	#4	#5	#6
Brazing temperatures	1440	1420	1350	1510	1525	1600

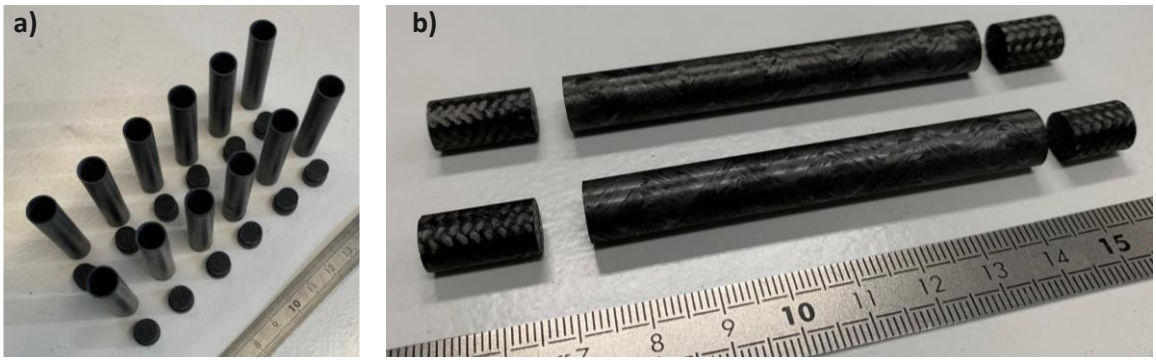

Figure 1: a) CVI-SiCf/SiC tubes and end-caps, b) representative specimens before brazing.

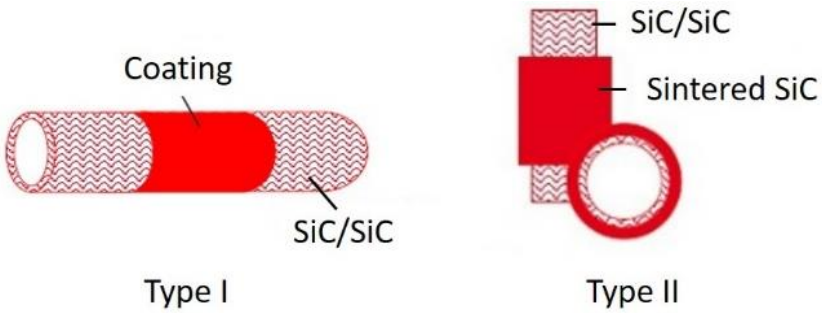

Figure 2: Schematic description of the specific samples (types I and II) for autoclave testing.

After brazing, the samples (Configurations A and C/Type II) were controlled by X-ray tomography (X-ray micro tomograph, GE 240 kV) to assess the filling of the joints by the braze. Mechanical tests by “push-out” were conducted on samples of configuration A. This method consists in applying a compressive force on the end-cap of the sample as illustrated in Figure 3. During the test, the compressive force (F) is measured, and the equivalent burst pressure (P_{burst}) and the nominal shear strength (σ_{NS}) are calculated according to the equations given in Figure 3.

Corrosion testing of selected samples (see Table 2) in an autoclave in under representative LWR water conditions (water+ steam, 360°C, 187 bars, 1000 ppm B) was performed for up to 64 days. After these experiments, all samples were examined visually and measured for mass loss. Scanning electron microscopy coupled with dispersive X-ray spectroscopy (EDXS) and X-ray diffraction techniques was performed on samples of configurations A and C/Type II.

Table 2: Sample and alloy references, remarks and number of days of exposure to autoclave (Tck_{joint}: joint thickness; H_{joint}: joint length (noted Hj on Figure 3).

Sample reference	Configuration	Braze reference	Remarks	Test in autoclave
No. 1	A	Alloy #1	Tck_{joint} ~ 85 µm, H_{joint} ~ 6 mm	24 days
No. 2	A	Alloy #1	Tck_{joint} ~ 105 µm, H_{joint} ~ 6 mm	No
No. 3	A	Alloy #1	Tck_{joint} ~ 85 µm, H_{joint} ~ 4.2 mm	No
No. 4	B	Alloy #1	H_{joints} ~ 6 mm	64 days
No. 5	C - type I	Alloy #2	-	28 days
No. 6	C - type I	Alloy #3	-	28 days
No. 7	C - type I	Alloy #4	-	42 days
No. 8	C - type I	Alloy #5	-	42 days
No. 9	C - type I	Alloy #6	-	24 days
No.10	C - type II	Alloy #2	Tck_{joint} ~ 200 µm, H_{joint} ~ 6 mm	28 days
No. 11	C - type II	Alloy #3	Tck_{joint} ~ 200 µm, H_{joint} ~ 6 mm	28 days

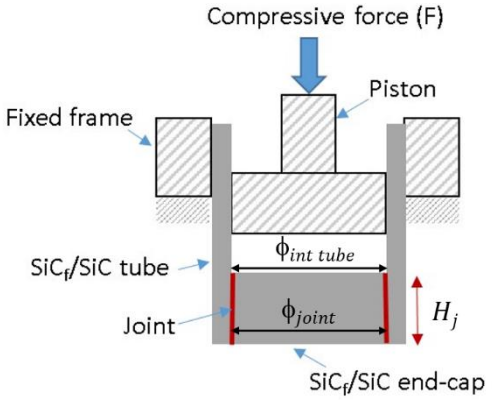

$$\sigma_{NJ} = \frac{F}{A_A} \quad \text{with} \quad A_A = H_j \pi \phi_{joint}$$

$$P_{burst} = \frac{F}{A_F} \quad \text{with} \quad A_F = \pi \frac{(\phi_{int\ tube})^2}{4}$$

Figure 3: Schematic description of the push-out test.

3. Results and discussion

Effect of ageing conditions in LWR environment reference BraSiC® braze Si-Zr alloy: Figure 4 shows a sample representative of Configuration A after brazing.

Figure 4: Sample N°1 brazed with the reference BraSiC® alloy.

Figure 5 (a)-(c) show X-ray tomography of sample No. 1 confirming the satisfactory filling of the joint region by the brazing material which appears white and grey in the images. Only a few areas

of the joint have a lack of braze (Figure 5b and c). While partial infiltration of the braze is observed significantly in the porosities of the end-cap and minimally in the tube, this infiltration did not occur to the detriment of the filling of the joint. Similar results were found for sample No. 3. In case of sample No. 2 (Figure 5d), there are more voids in the joint, due to the competition between infiltration of the liquid braze in the end-cap's porosities and the filling of the joint whose thickness (105 µm) is slightly higher than that of samples No. 1 (85 µm) and No. 2 (85 µm).

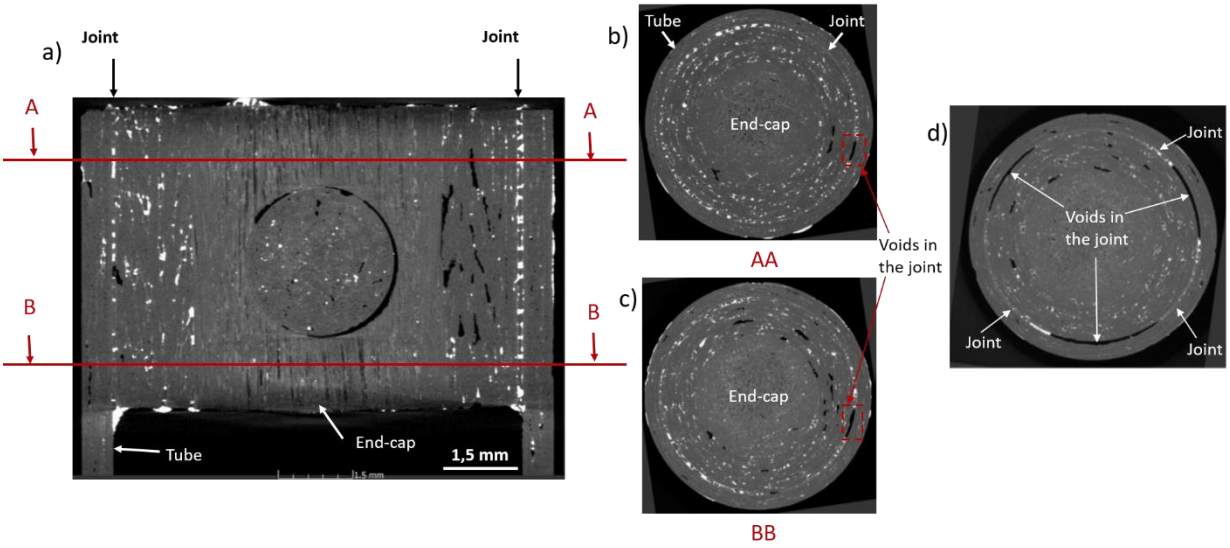

Figure 5: X-ray tomography control of samples after brazing: a), b) c) sample No. 1 and d) sample No. 2.

Sample No.1 was subjected to an autoclave testing in LWR water conditions for a period of 24 days. Following this test, no discernible change was observed on the sample although a slight mass loss was measured after the drying of the sample. It should be noted that no EBC was applied to this sample.

Subsequently, a series of mechanical push-out tests was carried out on samples No. 1, 2 and 3. No failure were observed in the joints. The failures seem to occur preferentially on the wall tubes near the brazed joint for all samples. Nevertheless, the damage initiation zones are not located (privileged site for crack nucleation that could be the joint or the interface braze / composite or the composite). Figure 6 presents the evolution of the compressive force F, as a function of displacement. The measured force at failure, and the calculated equivalent burst pressure and the shear strength at failure are provided in Figure 6. The shear strength at failure was lower for sample No. 1 (21 MPa), which was aged in autoclave prior to the push-out test. The shear strengths at failure are similar for samples No. 2 and 3 (respectively 29 and 30 MPa) whereas the forces at failure are different due to a difference in lengths between the joints (respectively 6 and 4.2 mm for samples No. 2 and 3). This result suggests that the length of brazed joint play a part in damage initiation.

After the mechanical tests, the joints were characterized by optical and scanning electron microscopy. Figure 7 depicts images of cross sections of sample No. 1. On the section perpendicular to the tube, the joint appears continuous (Figure 7a), exhibiting no lack of braze, and displaying a thickness that ranges from a few tens of micrometres to 100 µm (Figure 7a, b and c). Conversely, on the cross-section parallel to the tube (Figure 7d), the extremities of the joint are not totally filled by the braze which may have interacted with the water environment during the autoclave exposure in accordance with the slight loss of mass loss detected. The lack of braze

(not observed on sample No. 2 & 3) results in a reduction of the joint length from 6 mm to 4.2 mm (measured in cross-section of Figure 7d), which may be the cause of the observed reduction in shear strength as mentioned before. Indeed, considering the effective value of the joint length of sample No. 1 after test in autoclave (e.g., 4.2 mm), the corrected shear strength is 30 MPa, indicating that the mechanical properties of the remaining part of the joint are not degraded.
A microstructure analysis of the joint is presented in Figure 7b and reveals the presence of two distinct components: silicon (in grey) and silicide (in white). The presence of silicon, deemed to be not stable in LWR environment due to silica dissolution, may explain the braze interaction with LWR environment.
These results underscoring the need for continued attention to be paid to the oxidation of the brazing system.

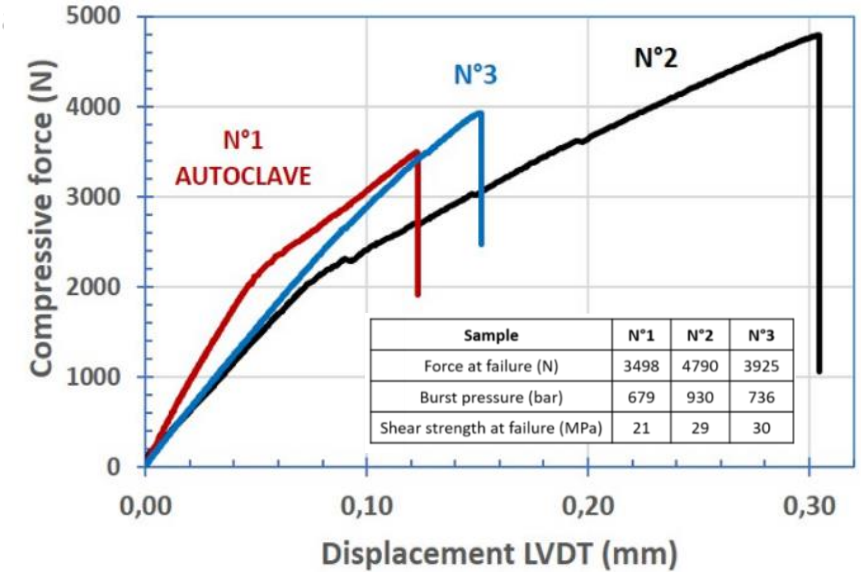

Figure 6: Evolution of the compressive force as a function of displacement during the push-out test and force, burst pressure and shear strength at failure measured from these tests on samples No. 1, 2 and 3 (for sample No. 1, the shear strength was calculated without taking into account the reduction of the joint length observed after test in autoclave).

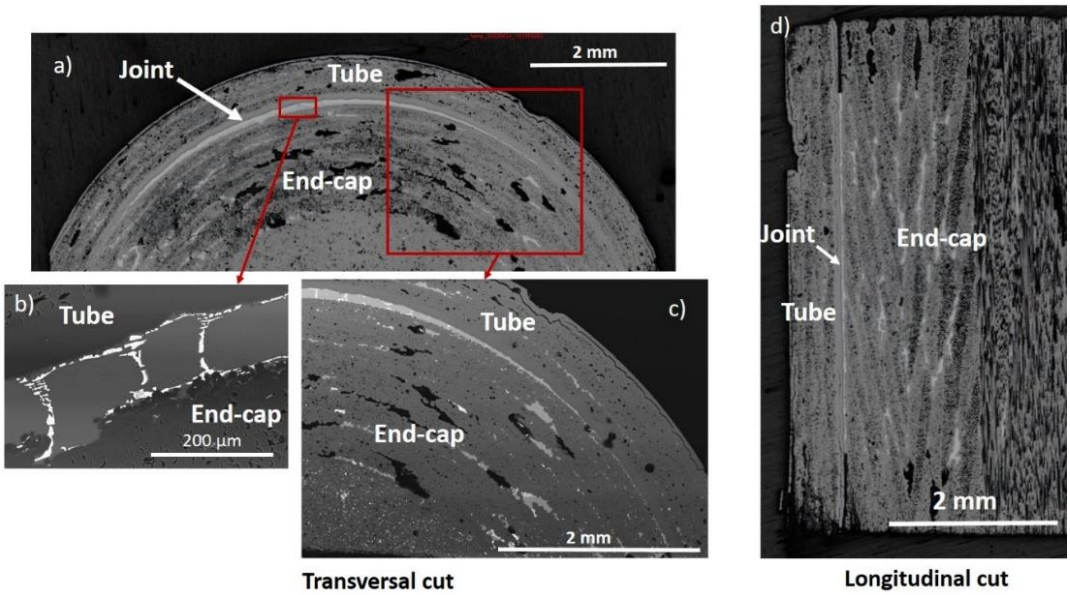

Figure 7: Optical micrographs (a) and d)) and SEM images (b) and c)) of sample N°1 after 24 days in autoclave and mechanical test.

Following these preliminary demonstration tests, the configuration B sample (Figure 8a) was prepared (an EBC-protected closed rodlet). Figure 8 shows the X-ray tomography of the configuration B sample. The brazing process effectively filled the joint (Figure 8b) with partial infiltration of the braze into the end-caps also observed.

The cladding tube, end-plug and brazed joint were coated by an EBC. Following 64 days of autoclave exposure, the specimen exhibited a golden colour, indicative of the formation of a submicronic protective oxide induced by the EBC. No other macroscopic changes were observed. The EBC effectively protected the SiC_f/SiC cladding, the SiC end-plug and the braze joints, with no measurable release of silicon into the autoclave 's water.

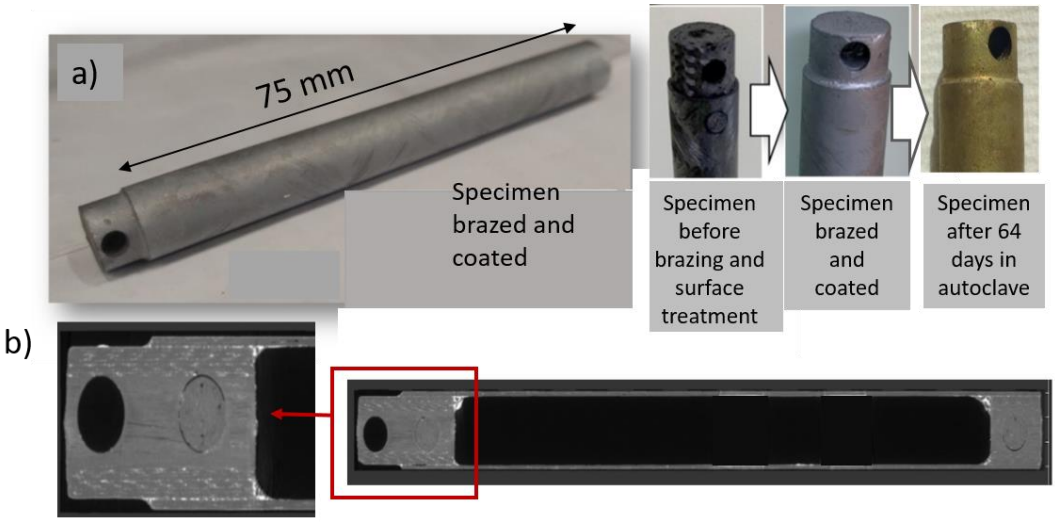

Figure 8: a) Visual aspects of representative specimen and b) X-ray tomography after brazing (longitudinal cut).

Optimised brazing alloy composition – While the EBC effectively protected the Si-Zr brazing material during 64 days of exposure, the observed reduction in the Configuration A's joint length during corrosion shows that the braze composition can be optimised further to prevent joint degradation in the event of defect in the EBC. Consequently, samples (No. 5 to No. 11) coated or brazed with various Si-Zr, Si-Cr, Si-Ti and Si-Y alloys were manufactured by CEA. Figure 9 shows samples coated with Si-Zr and Si-Cr alloys before and after 42 days of autoclave exposure. Following the test, colour changes were observed (white, grey and green colours), which are likely due to formation of different oxides, the exact nature of which is currently under investigation by X-ray diffraction.

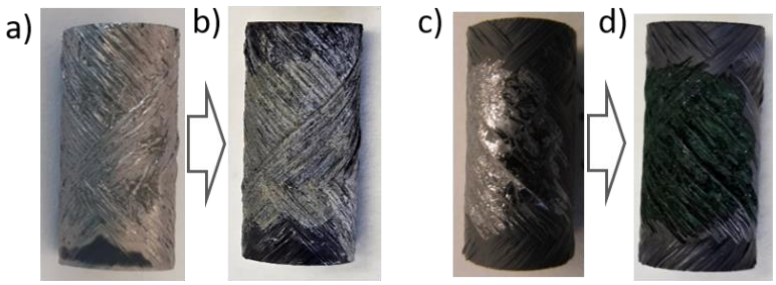

Figure 9: Example of changes of color for samples No. 5 and 6 respectively before a) and c), and after b) and d) test in autoclave.

The Si-Ti and Si-Y alloys (#6 and #5) were deemed unsuitable for further investigation as they exhibited mass losses of 3.3% after 24 days and 2.7% after 42 days, respectively. It can be noted, that even if the mass loss is calculated as the change in both brazing and SiC_f/SiC CMC mass, as demonstrated in reference [13] the mass loss of SiC_f/SiC composite after 24 days of autoclave exposure can be neglected.

The Si-Zr and Si-Cr (alloys #2 and #3) were subjected to further investigation in a joint configuration (Figure 2 Type II). The high joint thickness for these samples was higher than envisioned for a fuel rod (i.e., configuration B), which results in more penalising corrosion conditions. Their mass losses were measured to be significantly lower than those observed for Si-Ti and Si-Y alloys, with a minimum mass loss recorded ratio of 0.75%. Figure 10 and Figure 11 illustrate samples No. 10 and No. 11 (Si-Zr and Si-Cr respectively) before and after 28-days exposure period in autoclave. Following brazing, the joints were examined by X-ray tomography (Figure 10b and Figure 11b). This revealed a satisfactory filling of the braze despite a small lack of braze for sample No. 10. Upon examination of the samples after autoclave ageing, the integrity of these samples is observed (Figure 10c and Figure 11c), indicating that no separation occurred between cladding and end-cap. Furthermore, the microstructures of the joints were analysed using SEM (Figure 10d and Figure 11d) with EDS analysis. The extremities of the joints are still filled by a portion of the braze, which was previously partially transformed (by reaction with LWR environment). The nature of the products formed by interaction with water is under investigation. First results indicate the formation of a chromium oxide surrounding the silicide in sample No. 11 (Figure 11e). Further analyses are still in progress to evaluate the effect of 42 days in autoclave on the joints. Finally, other CVI-SiC_f/SiC brazed samples will be manufactured in more representative configuration (i.e., a CVI-SiC_f/SiC tube brazed with SiC/SiC end-cap and with a thinner brazing joint) for futher characterizations (like mechanical tests) and to allow a direct comparison with the reference Si-Zr alloy.

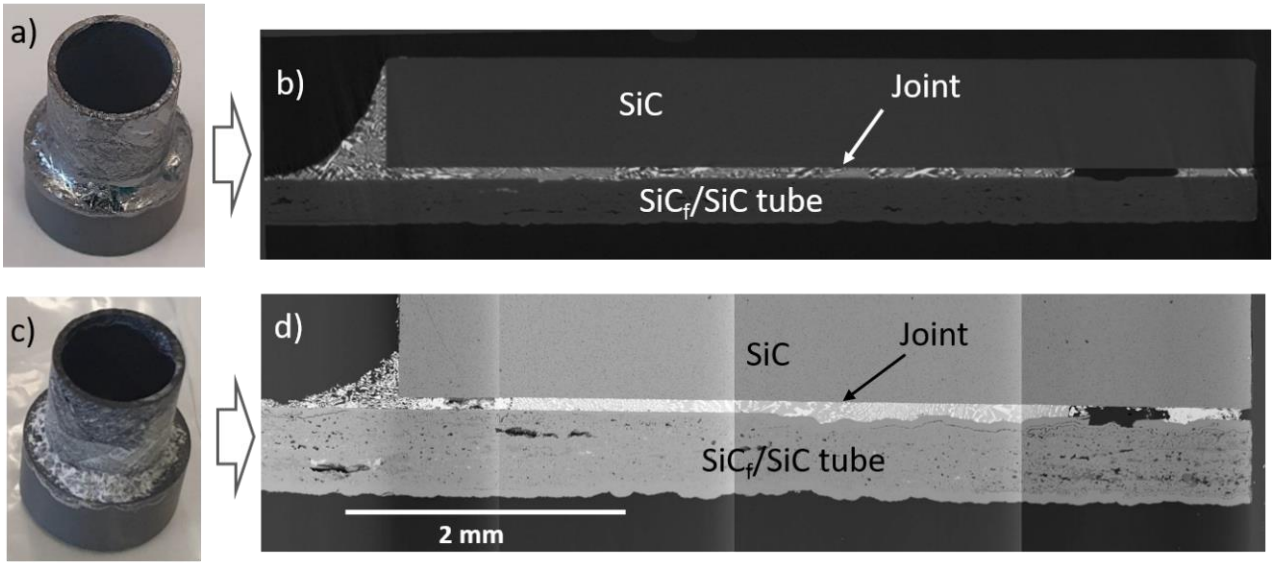

Figure 10: Observations of sample No. 10 a) before and c) after test in autoclave. Characterizations by b) X-ray tomography and d) SEM after autoclave exposure (28 days).

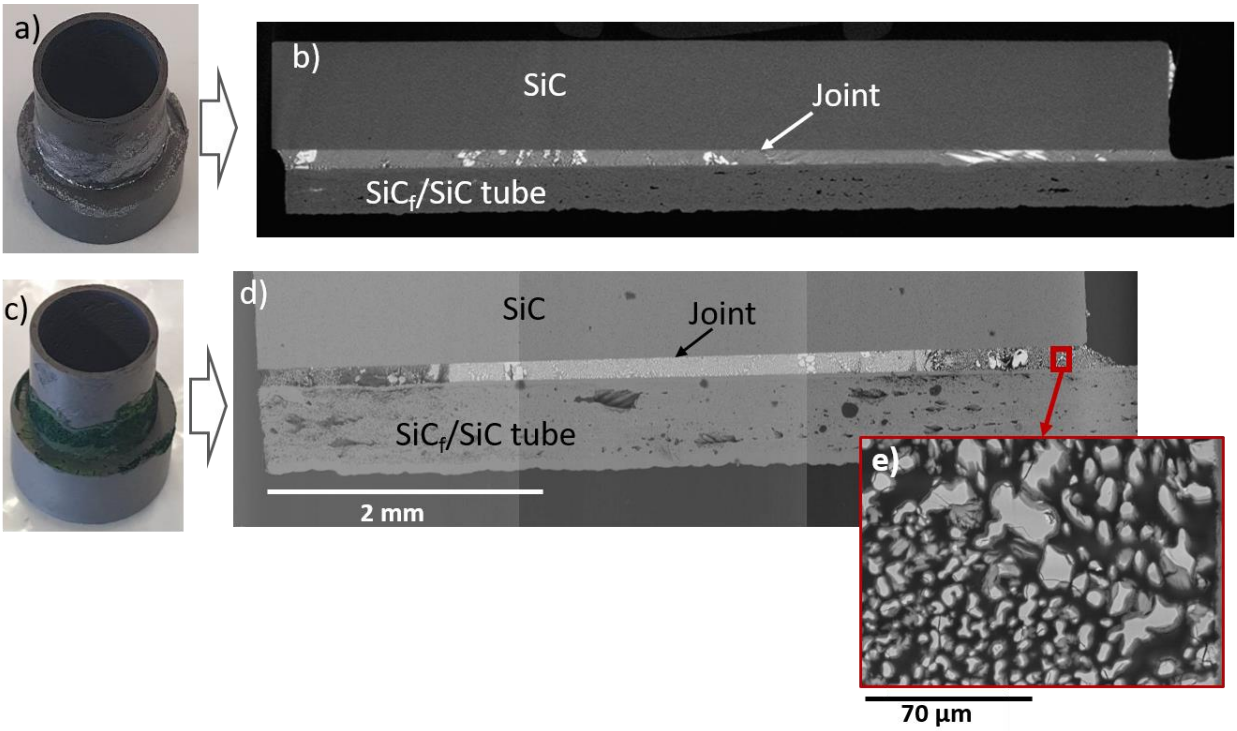

Figure 11: Observations of sample No. 12 a) before and c) after test in autoclave.

4. Summary and conclusions

This study was conducted through a collaborative work between Framatome and CEA and presents recent developments and investigations dedicated to the closure of tubular CVI-SiC_f/SiC samples using the BraSiC® process. Even if this brazing technology has already demonstrated its potential for various applications, its implementation in LWR requires addressing challenges, in particular to define a robust brazed joint capable of withstanding hydrothermal corrosion in LWR environment. The methodology used in this work is constituted of three steps and led to the following conclusions:

- Step 1: Brazing samples with a BraSiC® alloy (Si-Zr alloy #1) already specified for GFR and testing by push-out before and after exposure in autoclave. The results suggest that the LWR environment may affect the performance of the joints formed with the Si-Zr alloy, certainly due to a reduction of the joint length induced by interaction with the water environment;
- Step 2: Brazing with a Si-Zr alloy #1 of a representative 17x17 LWR rodlet protected by an EBC and corrosion testing in an autoclave. The EBC remained protective with no release of silicon detected in the autoclave water. Despite this favourable outcome, it would appear prudent to further optimise composition of the brazing alloy in order to mitigate the risk of EBC failure;
- Step 3: Autoclave screening tests with different BraSiC® alloys in two configurations (coating and joining). Some alloys led to high mass losses and are not recommended whereas those with low mass losses were analysed in joining configuration. Further investigation is now necessary to understand the interaction between the joint and the LWR environment in a representative geometry, as well as its effects on the joint to define a robust brazed joint.

5. Acknowledgments

The authors would like to thank Valérie Merveilleau and Carole Mollard (Univ. Grenoble Alpes, CEA, Liten, DTCH) for brazing and SEM/EDX analysis, Pierre Billaud and Guillaume Da Silva (Univ. Paris Saclay, CEA/DES-ISAS) for tests in autoclave, and James Braun (CEA/DAM-Le Ripault) for CVI-SiC/SiC production.

The French government has funded this research as part of the wider initiative known as the Plan de Relance. Some of the results have also been obtained in the PROtect-SiC programme, supported by the US-DOE.

6. References

[1] C. Nimishakavi, K; Sanders, B; Duquesne, L; Lorrette, "PROtect SiC: Framatome's Revolutionary ATF Solution for Improved Performance and Safety in LWRs," in *Top Fuel 2019, Seattle, WA, September 22-27, 2019*, 2019.

[2] L. Duquesne, K. Nimishakavi, and M. Aumand, "PROtect SiC – A revolutionary Enhanced Accident Tolerant Fuel design for improved performance and safety," in *Top Fuel 2021*,

[3] N. Vioujard, C. Lewis, W. Maxson, and J. Reed, "PROtect: The E-ATF solution by Framatome - overview of recent achievements and next steps," *Proc. TopFuel 2022 Light Water React. Fuel Perform. Conf.*, pp. 104–109, 2022, doi: 10.13182/TopFuel22-38976.

[4] A. Gasse, "Rôle des interfaces dans le brasage non réactif du SiC par les siliciures de Co et de Cu", Ph.D. thesis, Institut National Polytechnique de Grenoble, Grenoble, 1996.

[5] O. Mailliart, "Mouillage et brasage de SiC Sous atmosphère oxydante contrôlée par un alliage Co-Si et sous air par un mélange d'oxydes", Ph.D. thesis, Institut National Polytechnique de Grenoble, Grenoble, 2008.

[6] O. Mailliart, F. Hodaj, V. Chaumat, and N. Eustathopoulos, "Influence of oxygen partial pressure on the wetting of SiC by a Co-Si alloy," *Mater. Sci. Eng. A*, vol. 495, no. 1–2, pp. 174–180, 2008, doi: 10.1016/j.msea.2007.11.090.

[7] M. Lamy, "Etude structurale et chimique par Microscopie Electronique en Transmission d'interfaces SiC/siliciures de Co, Fe ou Ni", PH.D. thesis, Institut National Polytechnique de Grenoble, Grenoble, 2000.

[8] N. Eustathopoulos, M. G. Nicholas, and B. Drevet, *Wettability at high temperatures*, in R.W. Cahn (Ed.), Pergamon Materials series vol. 2. 1999.

[9] L. M. Nguyen, "Caractérisation mécanique de jonctions brasées SiC / BraSiC® / SiC et critère de dimensionnement à la rupture," 2011.

[10] V. Chaumat and G. Roux, "Multi-staged brazing using the BraSiC ® process for the fabrication of very large and / or complexe SiC based components .," in *International Conference on Brazing, High Temperature Brazing and Diffusion Bonding, Löt 2013*, 2013.

[11] D. M. A. Michaux, C. Sauder, J. Braun, M. Auclair, "Investigation Of The Neutron Irradiation Effects On The SiC/SiC Composites At High Temperature," *, ICC8 Conf. April 25-30, 2021*, p. 2021, 2021.

[12] C. Morel *et al.*, "The influence of grinding process on the mechanical behavior of SiC/SiC composite tubes under uniaxial tension," *J. Eur. Ceram. Soc.*, vol. 44, no. 1, pp. 91–106, 2024, doi: 10.1016/j.jeurceramsoc.2023.07.067.

[13] C. Lorrette, C. Sauder, P. Billaud, C. Hossepied, G. Loupias, et al. "SiC/SiC composite behavior in LWR conditions and under high temperature steam environment", Top Fuel 2015, Sep 2015, Zurich, Switzerland.